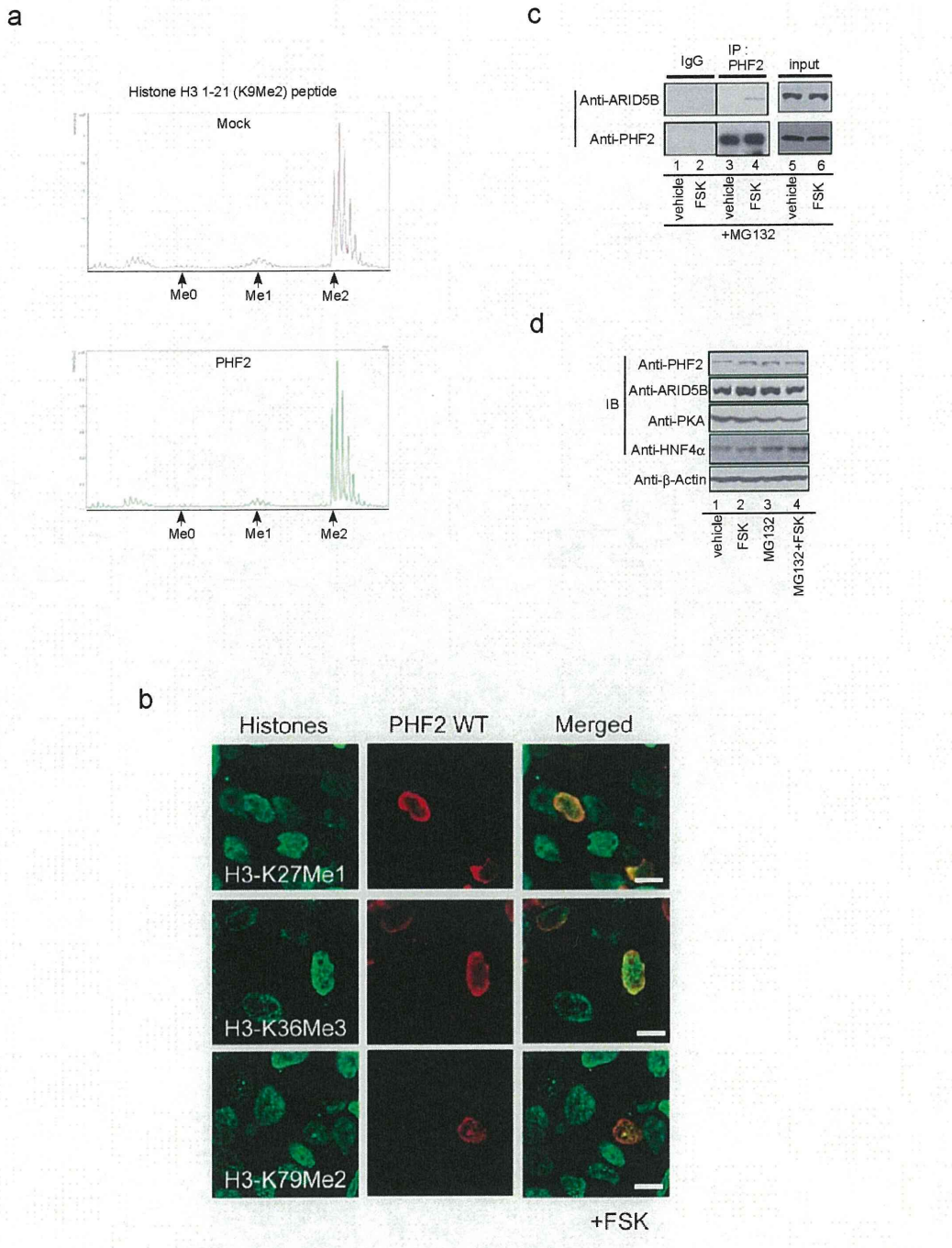

Figure S4 Demethylation activity of PHF2. **a,** Demethylase assay with H3 peptide. Purified PHF2 protein or mock immunoprecipitants incubated with PKA as in Fig. 3b was subjected to the demethylase assay with 0.2 μg of biotin-conjugated dimethyl histone H3 (Lys9) peptide (residues 1-21) (Upstate, 12-430). Demethylation was determined using MALDI-TOF/MS. Detailed methods were supplied as supplementary methods. **b,** Immunostaining of 293F cells was performed as described in Fig. 1f. **c,** Hepatocytes were treated with FSK (10^{-6} M) and MG132 (10^{-5} M) for two hrs. Total cell lysates were subjected to immunoprecipitation as indicated. **d,** FSK treatment did not alter protein expression levels of PHF2, ARID5B, or HNF-4α. Hepatocytes were treated with FSK (10^{-6} M) or MG132 (10^{-5} M) as indicated for 6 hrs. Cell lysates were subjected to Western blotting.

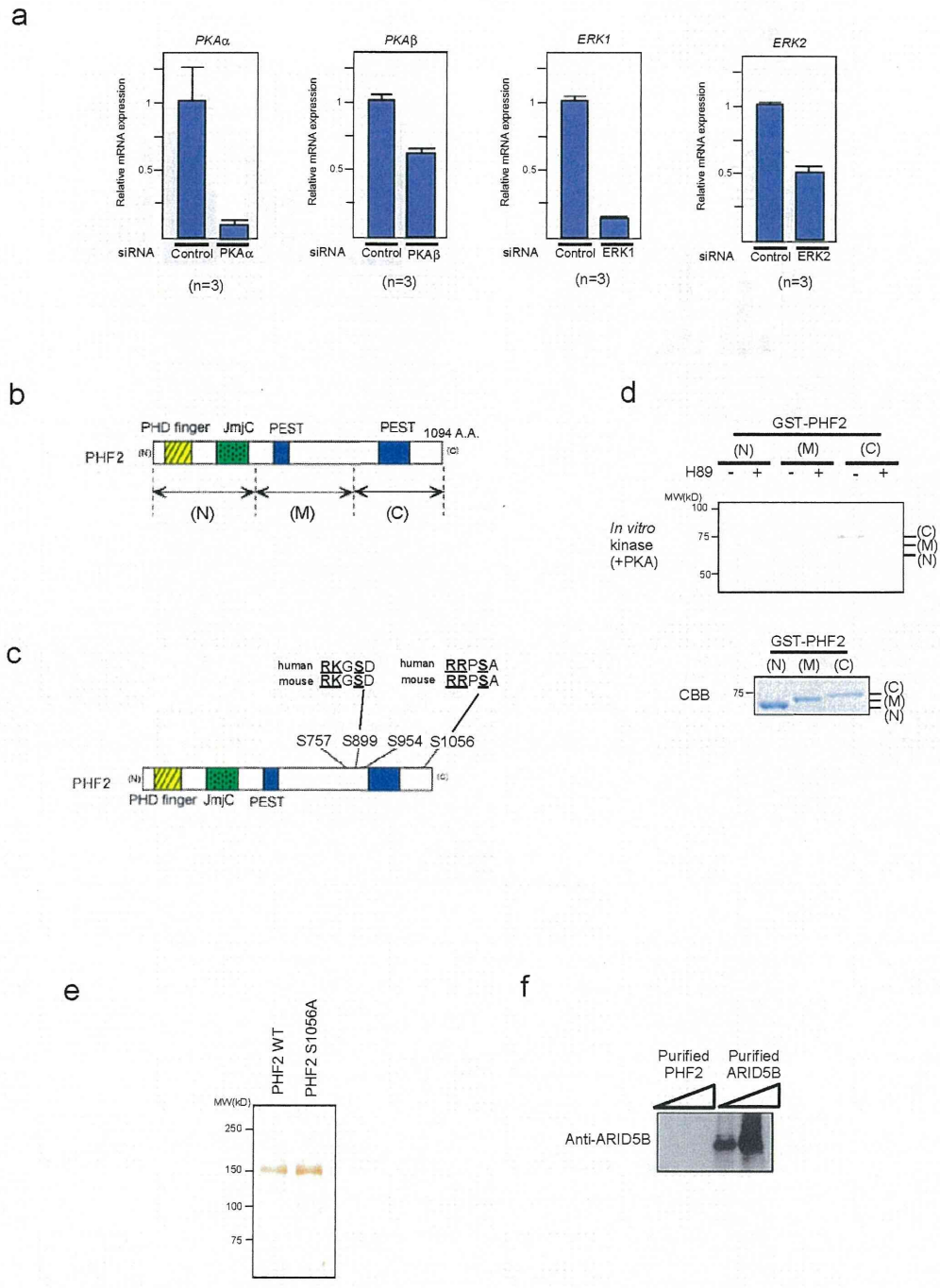

Figure S5 PKA phosphorylates PHF2 *in vitro* and *in vivo*. **a**, As controls for Fig. 2d, expression levels of the indicated genes were quantified by qPCR. Data shows average +/-S.D. (n=3). **b**, The schematic representation of deletion mutants of PHF2 used. **c**, The schematic representation of phosphorylation sites within PHF2 determined in Figure 2. **d**, PHF2 is phosphorylated by PKA at C-terminal region *in vitro*. *In vitro* kinase assay as indicated. **e**, 293F cells were transfected with FLAG-PHF2 or its mutant, and PHF2 was purified to of near homogeneity using anti-FLAG affinity column. Purified proteins were subjected to silver staining as indicated. **f**, Purified protein in Fig. 3a were subjected to Western blotting. Note that purified PHF2 did not include ARID5B.

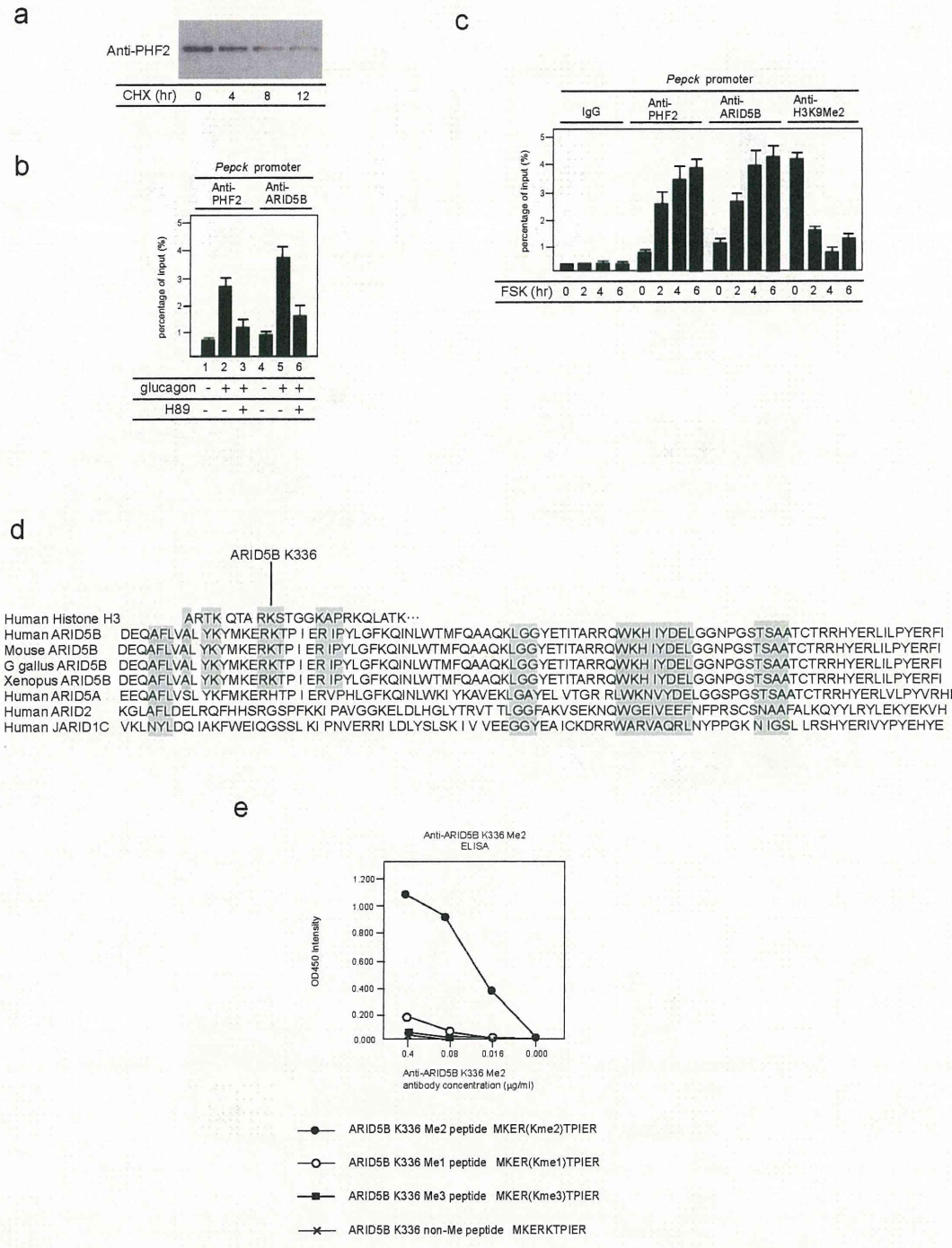

Figure S6 Promoter recruitment of PHF2/ARID5B. **a**, Protein turn-over of PHF2 as revealed by cycloheximide treatment. **b**, Recruitment of PHF2 and ARID5B to the *Pepck* promoter was abolished by a PKA inhibitor, H89. Hepatocytes were treated with glucagon and/or H89 (1 μM) for four hrs, then ChIP assay was performed using the indicated antibodies. **c**,, Co-recruitment of PHF2/ARID5B and demethylation of H3K9Me2 in *Pepck* promoter over similar time courses. Hepatocytes were treated with FSK for the indicated time, then a ChIP assay was performed as indicated. **d**, The schematic representation of amino acid sequences of ARID5B and other ARID family proteins. The sequence of histone H3K9 is also represented. **e**, Specificity of anti-ARID5B K336Me2 antibody. A rabbit polyclonal antibody against di-methylated Lys336 of ARID5B (anti-ARID5B K336Me2) was raised by using the di-methylated peptide [ARID5B K336Me2; MKER(Kme2)TPIER], and purified over a peptide-affinity column. The specificity of antibody toward K336Me2 peptide over non-methylated, mono-methylated, or tri-methylated peptides was determined by ELISA assays.

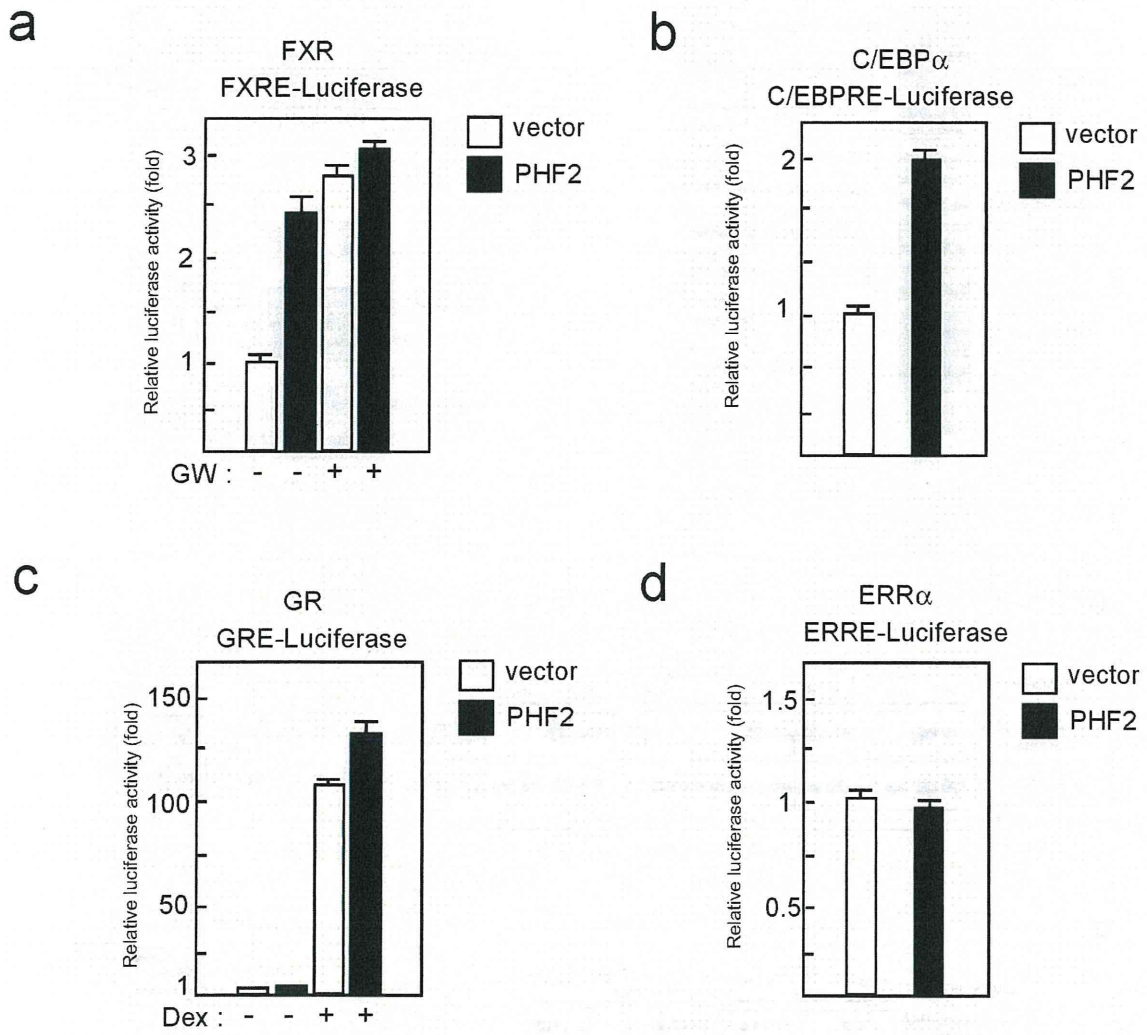

Figure S7 Co-activator activity of PHF2 for known gluconeogenic-related transcription factors. 293F cells were transfected with the indicated expression vectors and reporter plasmids with or without PHF2. Cells were treated with FSK for 24 hrs, then Luciferase assay were performed as indicated.

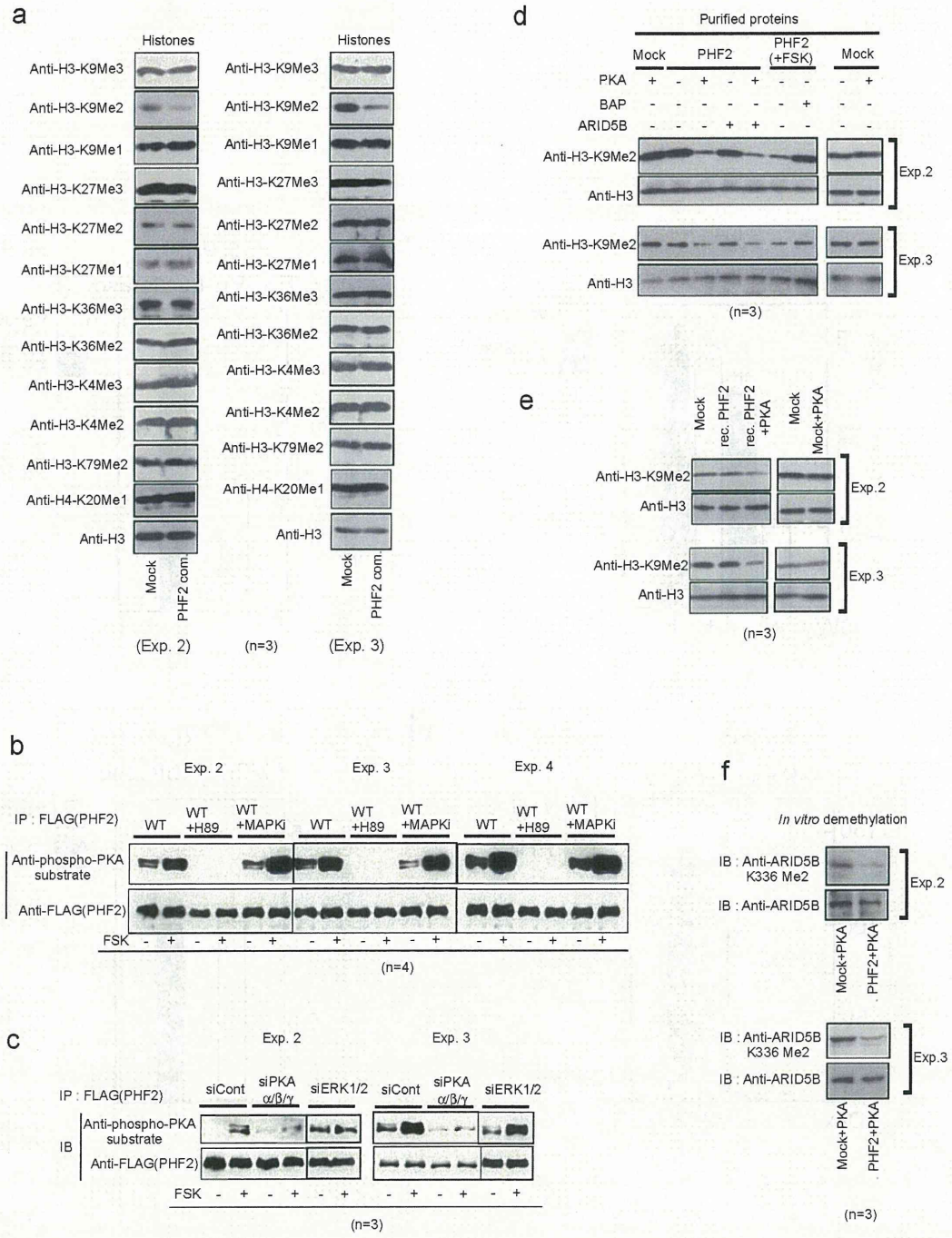

Figure S8 Western blot data for quantification. **a**, For *in vitro* demethylation assay and quantification in Fig. 1c-d, three independent experiments were performed, and histone methylation marks were analyzed by Western blotting as shown in Fig. 1d. The other two sets of data for quantification are shown. **b-c,** Quantification analysis for PKA-mediated phosphorylation of PHF2. Assay was performed as in Fig. 2d, and the other data for quantification in Fig. 2d (left, n=4 and right, n=3) were shown. **d-e**, Quantification analysis for PKA-dependent PHF2 demethylase activity. Three independent assays were performed as in Fig. 3b-c and 3e-f, and the other two sets of data for quantification (n=3) were shown. **f**, Quantification analysis for demethylation of ARID5B by PHF2 *in vitro*. Three independent assay was performed as in Fig. 5e, and the other two sets of data for quantification in the lower panel of Fig. 5e (n=3) were shown.

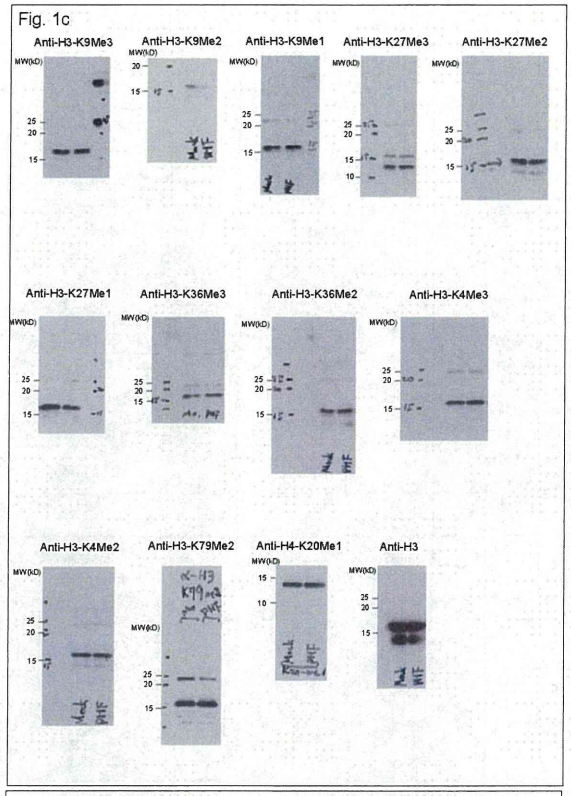

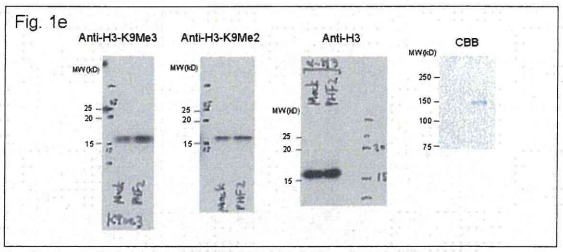

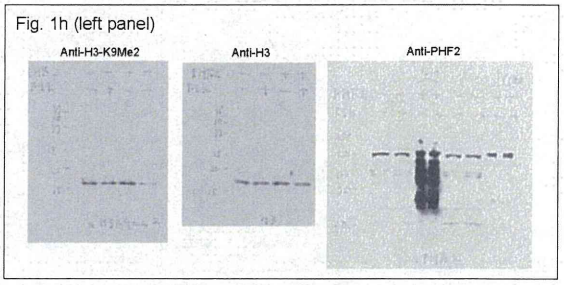

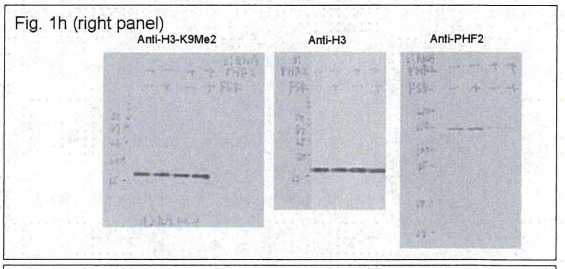

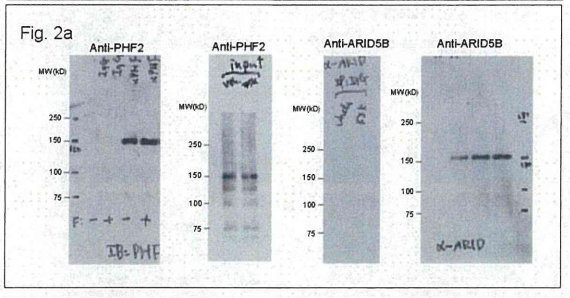

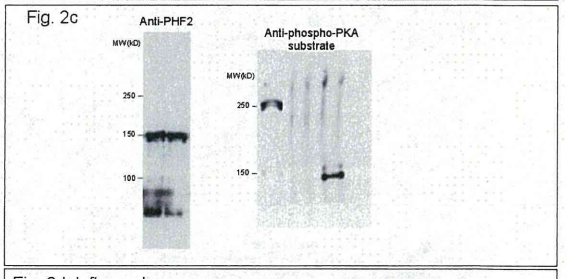

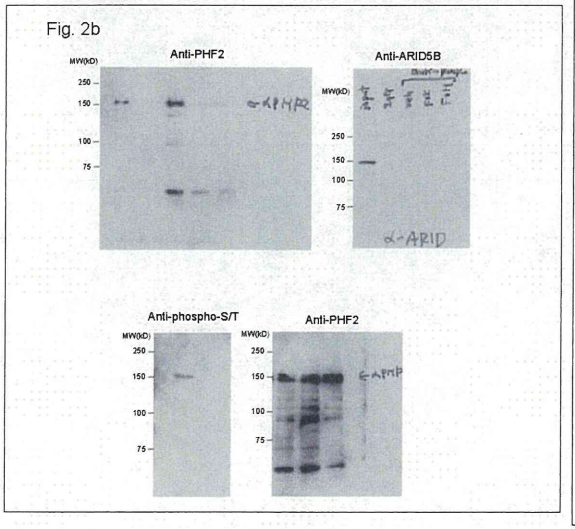

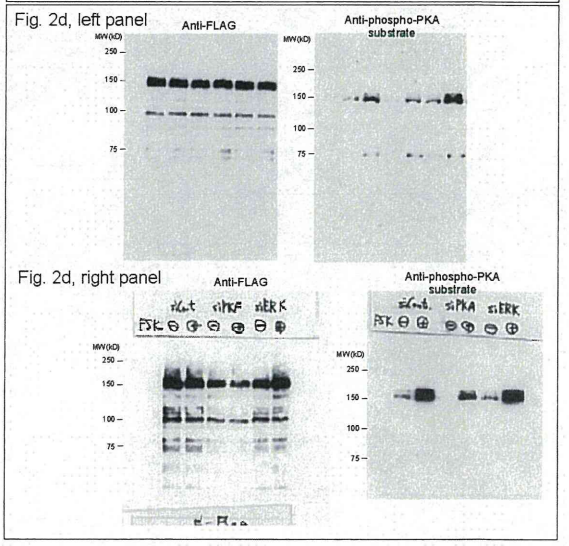

Figure S9 Full scans

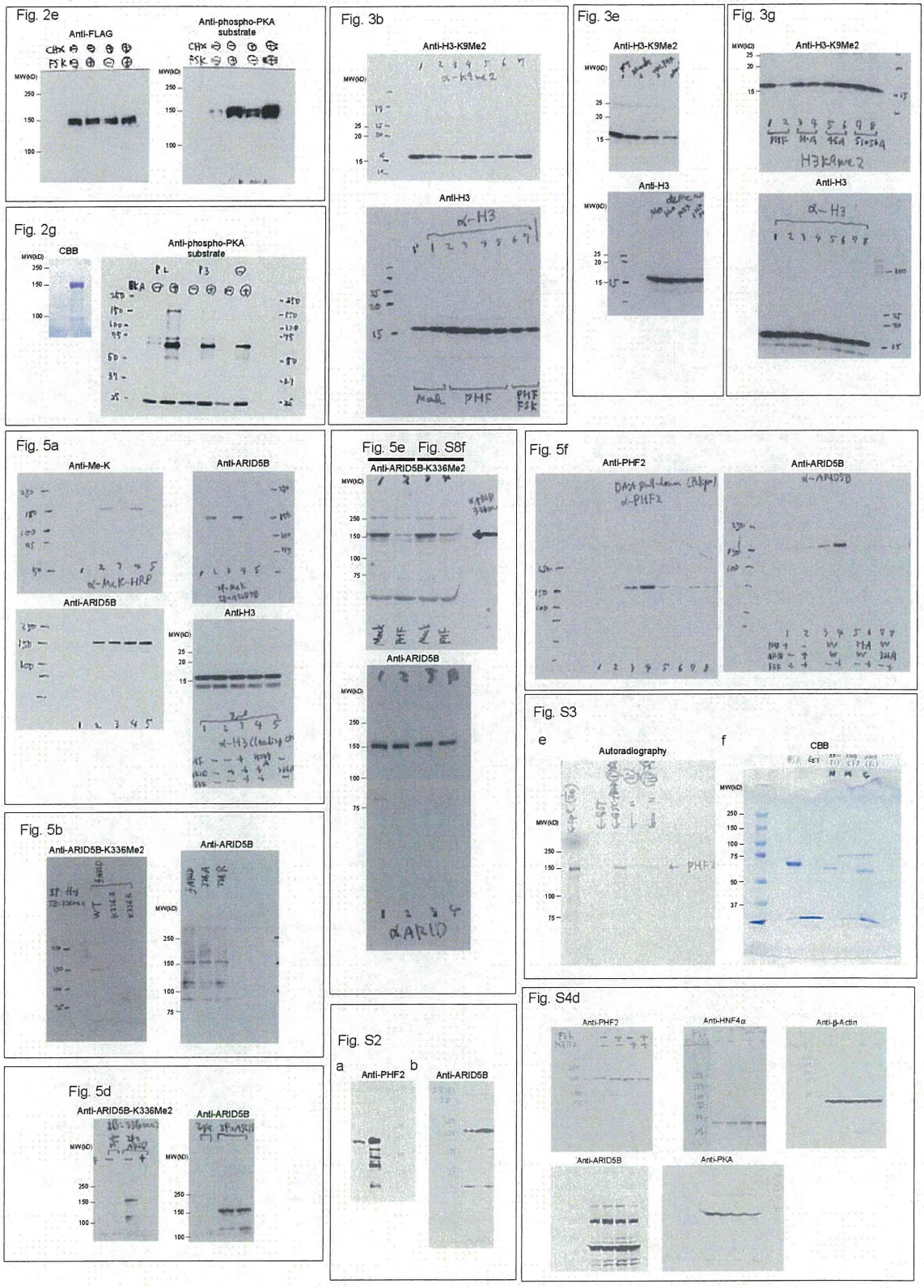

Figure S9 continued

Supplementary Table 1

Lists of antibodies, primers, and siRNA sequences used in this study.

Antibodies for immunoprecipitation

Antibody	Manufacture	Catalag No.	Lot No.
HNF4	Santa Cruz	H-171	K0204
FXR	Santa Cruz	H-130	K2805
FLAG M2	Sigma	F1804	088K6018
PHF2	Our laboratory		
ARID5B	Our laboratory		

Antibodies for Western blotting

Antibody	manufacture	Catalog No.	Lot No.	dilution
PHF2	Our laboratory			1/1000
ARID5B	Our laboratory			1/1000
FXR	Santa Cruz	sc1204	B052	1/500
RXRα	Santa Cruz	D-20	L210	1/1000
methyl-lysine	Abcam	ab23367	458685	1/300
FLAG	Sigma	F-7425	069K4767	1/1000
HA	Immunology Consultants Laboratory	RHGT-45A-4	22	1/1000

Antibodies for histone modification

Antibody	manufacture	Catalog No.	Lot No.	dilution
H3K9Me3	Abcam	ab6001	641998	1/1000
H3K9Me2	Abcam	1220	764743	1/1000
	Upstate	07-441	DAM1463717	1/1000
H3K9Me1	Upstate	07-450	DAM1394811	1/1000
H3K27Me3	Upstate	07-449	DAM1421462	1/1000
H3K27Me2	Upstate	07-452	24461	1/1000
H3K27Me1	Upstate	07-448	24439	1/1000
H3K4Me3	Upstate	07-473	131172	1/1000
H3K4Me2	Upstate	07-030,	DAM15170816	1/1000
H3K36Me3	Abcam	9050	826245	1/1000
H3K36Me2	Upstate	07-369	22475	1/1000
H3K79Me2	Abcam	ab3594	62690	1/1000
H4K20Me1	Upstate	07-748	30587	1/1000
H3	Abcam	ab1791	940500	1/2000

Primers for ChIP

mouse *Pepck* promoter	Fw	5'- TGTGCAGCCAGCAACATATGAA -3'
	Rv	5'- TGCAGGCTCTTGCCTTAATTGTC -3'
mouse *G6Pase* promoter	Fw	5'- GTCAAGCAGTGTGCCCAAGTTAATA -3'
	Rv	5'- CCCAGCCCTGATCTTTGGAC -3'
mouse *Gapdh* promoter	Fw	5'- CCTGCTTATCCAGTCCTAGCTCA -3'
	Rv	5'- AAATGAGGCGGGTCCAAAG -3'

Primers for Realtime RT-qPCR

mouse *Pepck*	Fw	5'- GTGTTTGTAGGAGCAGCCATGAGA -3'
	Rv	5'- GCCAGGTATTTGCCGAAGTTGTAG-3'
mouse *G6Pase*	Fw	5'- GGATCCTGGGACAGACACACAA-3'
	Rv	5'- TGTCAACACCTCTGGCCTCAC -3'
mouse *Hnf4a*	Fw	5'- CCGGGTGTCAGGAACAGTTG -3'
	Rv	5'- TGCAGGACAGTCTGAGCCATC -3'
mouse *Gapdh*	Fw	5'-AAATGGTGAAGGTCGGTGTG -3'
	Rv	5'-TGAAGGGGTCGTTGATGG -3'

Sequences of siRNA

mouse PHF2	#1	5'-CAGCAAACCUGACUCGUUAUU -3'
	#2	5'-GCAAAGGCUUGGAAAGAUCUU -3'
mouse ARID5B	#1	5'-CCAAUCAUUUGACAUGUUCUU -3'
	#2	5'-UCACAUGGGCGCAUUCUGAUU -3'
human PHF2	#1	5'- GCAAGCGCCUGACGUCAAG -3'
	#2	5'- AGGAGUUUGUGGACUAUUA -3'
human ARID5B	#1	5'- UAACGGACCAGUUUGCAUU -3'
	#2	5'- GCAGUCAACCCUAAACAGU -3'
mouse HNF4α	#1	5'- GAAGGAAGCUGUCCAAAAU -3'
	#2	5'- AGAGGUCCAUGGUGUUUAA -3'

BIOLOGY OF REPRODUCTION 84, 734–742 (2011)
Published online before print 1 December 2010.
DOI 10.1095/biolreprod.110.087502

Endocrine Disrupter Bisphenol A Increases In Situ Estrogen Production in the Mouse Urogenital Sinus[1]

Shigeki Arase,[3,5] Kenichiro Ishii,[3,4,5] Katsuhide Igarashi,[6] Kenichi Aisaki,[6] Yuko Yoshio,[5] Ayami Matsushima,[7] Yasuyuki Shimohigashi,[7] Kiminobu Arima,[5] Jun Kanno,[6] and Yoshiki Sugimura[2,5]

Department of Nephro-Urologic Surgery and Andrology,[5] Mie University Graduate School of Medicine, Mie, Japan
Division of Cellular & Molecular Toxicology,[6] National Institute of Health Sciences, Tokyo, Japan
Laboratory of Structure-Function Biochemistry,[7] Department of Chemistry, Faculty of Sciences, Kyushu University, Fukuoka, Japan

ABSTRACT

The balance between androgens and estrogens is very important in the development of the prostate, and even small changes in estrogen levels, including those of estrogen-mimicking chemicals, can lead to serious changes. Bisphenol A (BPA), an endocrine-disrupting chemical, is a well-known, ubiquitous, estrogenic chemical. To investigate the effects of fetal exposure to low-dose BPA on the development of the prostate, we examined alterations of the in situ sex steroid hormonal environment in the mouse urogenital sinus (UGS). In the BPA-treated UGS, estradiol (E_2) levels and CYP19A1 (cytochrome P450 aromatase) activity were significantly increased compared with those of the untreated and diethylstilbestrol (DES)-treated UGS. The mRNAs of steroidogenic enzymes, *Cyp19a1* and *Cyp11a1*, and the sex-determining gene, *Nr5a1*, were up-regulated specifically in the BPA-treated group. The up-regulation of mRNAs was observed in the mesenchymal component of the UGS as well as in the cerebellum, heart, kidney, and ovary but not in the testis. The number of aromatase-expressing mesenchymal cells in the BPA-treated UGS was approximately twice that in the untreated and DES-treated UGS. The up-regulation of *Esrrg* mRNA was observed in organs for which mRNAs of steroidogenic enzymes were also up-regulated. We demonstrate here that fetal exposure to low-dose BPA has the unique action of increasing in situ E_2 levels and CYP19A1 (aromatase) activity in the mouse UGS. Our data suggest that BPA might interact with in situ steroidogenesis by altering tissue components, such as the accumulation of aromatase-expressing mesenchymal cells, in particular organs.

aromatase, bisphenol A, developmental biology, embryo, estradiol/estrogen receptor, in situ estrogen production, male reproductive tract, prostate, steroidogenic enzyme, urogenital sinus

[1]Supported by Grants-in-Aid from the Ministry of Health, Labor, and Welfare, Japan. GEO accession no. GSE24928.
[2]Correspondence: Yoshiki Sugimura, Department of Nephro-Urologic Surgery and Andrology, Mie University Graduate School of Medicine, 2-174 Edobashi, Tsu, Mie 514-8507, Japan. FAX: 81 59 231 5203; e-mail: sugimura@clin.medic.mie-u.ac.jp
[3]These authors contributed equally to this work.
[4]Current address: Mie University Graduate School of Regional Innovation Studies, 1577 kurimamachiya-cho, Tsu, Mie 514-8507, Japan.

Received: 27 July 2010.
First decision: 19 August 2010.
Accepted: 15 November 2010.

eISSN: 1529-7268 http://www.biolreprod.org
ISSN: 0006-3363

INTRODUCTION

Endocrine-disrupting chemicals (EDCs) have been implicated in the alteration of fetal development of urogenital organs as well as the reproductive and endocrine systems in humans and other species [1]. The fetal development of urogenital organs is induced by endogenous hormonal messages that originate in fetal and maternal hormone systems. Fetal exposure to EDCs disrupts the interactions between endogenous hormones and their receptors, causing adverse effects later in life [2]. In the prostate, both androgens and estrogens play a significant role in development and differentiation as well as in the maintenance of adult homeostasis [3]. Therefore, even small changes in estrogen levels, including those of estrogen-mimicking chemicals, can lead to changes in prostate development and differentiation.

Bisphenol A (BPA), one of the EDCs, is a well-known, ubiquitous, estrogenic chemical used in the manufacture of polycarbonate plastics, as a lining in metal food and drink cans, and in dental sealants [4]. The concern with BPA originates from its detection in maternal and fetal plasma as well as the placenta [5, 6]. Thus, fetal exposure to BPA is implicated in fetal toxicity as well as in subsequent growth of the infant. Histopathologically, fetal exposure to low-dose BPA (10 μg kg^{-1} day^{-1}) has been shown to increase cell proliferation of urogenital sinus epithelium (UGE) in the primary prostatic ducts of CD1 mice [7]. Recently, our group reported that fetal exposure to low-dose BPA (20 μg kg^{-1} day^{-1}) specifically increased the number of basal epithelial cells in the adult prostate of BALB/c mice and also induced permanent cytokeratin 10 expression in such cells similar to the effects of synthetic estrogen diethylstilbestrol (DES; 0.2 μg kg^{-1} day^{-1}) [8]. Epigenetically, neonatal exposure of male rats to low-dose BPA (10 μg kg^{-1} day^{-1}) elicited critical molecular changes during prostate development and also increased prostatic gland susceptibility to precancerous neoplastic lesions and hormonal carcinogenesis [9]. Toxicological studies of BPA at less than 50 μg kg^{-1} day^{-1} in rodent fetuses and offspring have demonstrated alterations of mammary gland development, open-field behavior, and reproductive functioning [10–12].

Some EDCs are reported to alter the in situ sex steroid hormonal environment in the reproductive system. The triazine herbicide atrazine binds directly to adrenal-4-binding protein/steroidogenic factor-1 (official symbol NR5A1) and increases CYP19A1 (cytochrome P450 aromatase) expression and, ultimately, estradiol (E_2) production in human genital cancer cell lines [13]. The aryl hydrocarbon (dioxin) also increases CYP19A1 (aromatase) expression mediated by its receptor in mouse ovaries [14]. In contrast, the phosphorothioate insecticide profenofos increases the expression of steroidogenic genes

and testosterone levels in rat testes [15]. Recently reported adverse effects of BPA on in situ steroidogenesis include increased testosterone levels in mouse Leydig cells and decreased E_2 levels in porcine ovarian granulosa cells [16, 17]. Thus, BPA may have the potential not only to mimic estrogenic action but also to alter in situ steroidogenesis in the prostate as well as other reproductive organs.

To investigate the effects of fetal exposure to low-dose BPA on in situ steroidogenesis in the developing prostate, we first measured sex steroid hormone levels and CYP19A1 (aromatase) activity in the BPA-treated mouse urogenital sinus (UGS), from which the prostate develops embryologically. Subsequently, we examined the alterations of steroidogenic enzyme gene expression to confirm the alterations of the in situ sex steroid hormonal environment in the BPA-treated mouse UGS. Finally, we identified the BPA-specific biological effects for in situ steroidogenesis during fetal prostate development.

MATERIALS AND METHODS

Animals

In the present study, 36 pregnant female C57BL/6 mice were purchased on the 12th day of gestation from Japan SLC, where the breeding strategy was to mate three female C57BL/6 mice (age, 10 wk) with one male overnight and separate them the next morning (plug date denoted as Day 0). All animals were housed individually in chip-bedded polyolefin cages in a room with controlled temperature (23 ± 1°C) and humidity (45 to 65%) on a 12L:12D photoperiod. Mice were fed a low-phytoestrogen diet (NIH-07PLD; Oriental Yeast Co.) and tap water ad libitum.

Chemicals

For the present study, both BPA and DES with a purity of 99% or greater were purchased from Nacalai Tesque and Wako Pure Chemical Industries, respectively.

Fetal Exposure to Chemicals

We randomly assigned 36 pregnant female C57BL/6 mice to three different treatment groups: BPA (20 $\mu g\ kg^{-1}\ day^{-1}$, n = 12) or DES (0.2 $\mu g\ kg^{-1}\ day^{-1}$, n = 12), both of which were dissolved in tocopherol-stripped corn oil (MP Biomedical, Inc.), administered by oral gavages on Embryonic Day (E) 13 to E16 and the control group, in which pregnant mice were fed tocopherol-stripped corn oil (2 ml/kg, n = 12). Previously, our group reported that this protocol of fetal exposure to BPA and DES resulted in similar histopathological changes of adult prostate—that is, increased basal epithelial cell number and induction of cytokeratin 10, a classic marker associated with squamous differentiation, in such cells [8]. Our dose level of BPA for the present study was also based on reported results suggesting that BPA is less than 100-fold less potent than DES. The Mie University's Committee on Animal Investigation approved the experimental protocol.

Termination and UGS Dissection

Between E17 and Postnatal Day (P) 1, all animals were terminated by an overdose of isoflurane followed by cervical dislocation. For each of the three groups, from 15 to 18 fetuses (both male and female) from three pregnant mice were collected at E17, E18, P0, and P1. The bladder and urethra were removed and dissected to isolate the UGS, and then the five or six UGS obtained were pooled as one sample. Thus, the 15–18 UGS were divided into three samples at each time point. The UGS, cerebellum, heart, kidney, testis, and ovary were collected in RNAlater (Applied Biosystems).

To isolate pure UGS, other tissues, such as the bladder, urethra, wolffian duct, seminal vesicle, and mullerian duct, were removed from both the male and female urogenital tracts. The histopathology of the mouse UGS was then examined by hematoxylin-and-eosin staining.

Measurements of In Situ E_2 Levels and CYP19A1 (Aromatase) Activity in UGS

The E_2 levels and CYP19A1 (aromatase) activity in UGS were determined by liquid chromatography-tandem mass spectrometry [18] and a tritiated water release assay [19], respectively, which were made available by Aska Pharma Medical. Briefly, the organs were homogenized, and the extracts were applied to a C18 Amprep solid-phase column (Amersham Biosciences) to remove contaminating fats. The E_2 was then separated using a normal-phase high-performance liquid chromatography system (Jasco) with a silica gel column (Cosmosil 5SI; Nacalai Tesque), and 100 pg of isotope-labeled $[^{13}C_4]E_2$ were added to extracts. The evaporated extracts were reacted with 5% pentafluorobenzyl bromide/acetonitrile, under KOH/ethanol, for 1 h at 55°C. After evaporation, the products were reacted with 100 ml of picolinic acid solution (2% picolinic acid, 2% 2-dimethylaminopyridinc, and 1% 2-methyl-6-nitrobenzoic acid in tetrahydrofuran) and 20 ml of triethylamine for 0.5 h at room temperature. The reaction products were dissolved in 1% acetic acid and then purified using a Bond Elute C18 column (Varian). The products were measured with a reverse-phase liquid chromatograph (Agilent 1100; Agilent Technologies) coupled with an API 5000 triple-stage quadrupole mass spectrometer (Applied Biosystems) in the positive-ion mode. This device monitored the *m/z* 558 to *m/z* 339 (E_2) and *m/z* 562 to *m/z* 343 ($[^{13}C_4]E_2$) transitions.

The tritiated water release assay was used for the measurement of CYP19A1 (aromatase) activity. This method measures the production of ^3H_2O, which forms as a result of aromatization of the substrate [1b-^{3}H]androst-4-ene-3,17-dione (New England Nuclear). Serum-free medium containing [1b-^{3}H]androst-4-ene-3,17-dione solution (54 nM) was prepared, of which 0.5 ml was added to each sample. After incubation for 1 h, the samples were placed on ice, and 200 µl of culture medium were withdrawn. The medium was extracted with 500 µl of chloroform, vortexed, and then centrifuged for 1 min at 9000 × *g*. A 100-µl aliquot of the aqueous phase was mixed with 100 µl of a 5% (wt/vol) charcoal/0.5% (wt/vol) dextran T-70 suspension, vortexed, and then incubated at room temperature for 10 min. Then, after centrifugation of the solution for 5 min at 9000 × *g*, a 150-µl aliquot was removed for measurement of radioactivity by liquid scintillation.

RNA Extraction and cDNA Preparation

Total RNA was extracted using the RNeasy Mini Kit (Qiagen, Inc.) in accordance with the manufacturer's instructions. The RNA concentration was then determined spectrophotometrically by a multidetection microplate reader (Dainippon Sumitomo Pharma Co.). From 50 ng of total RNA, cDNA was reverse transcribed using oligo(dT) and Superscript II RNase H-reverse transcriptase (Invitrogen) as previously described [8].

Analysis of Gene Expression Profile

For determining gene expression profiles of the male UGS, GeneChip analysis with the Percellome method was performed [20]. Briefly, organs were prepared using RLT buffer (Qiagen, Inc.). Total RNA was extracted using RNeasy Mini Kit. First-strand cDNA was synthesized by incubating 5 mg of total RNA with a T7 oligo(dT) primer (Invitrogen) according to the manufacturer's protocol. The dsDNA was mixed with T7 RNA polymerase (Enzo Biochem, Inc.). During the in vitro transcription, generated cRNAs were labeled with biotin-16-UTP and biotin-11-CTP (Enzo Biochem, Inc.). The purified cRNA was fragmented at 300–500 bp into the target solution. Hybridization was performed with the GeneChip Mouse Genome 430 Version 2.0 (Affymetrix, Inc.) at 45°C for 18 h after staining with streptavidin-R-phycoerythrin conjugates (Molecular Probes, Invitrogen). The reacted arrays were then scanned as digital image files, and the scanned data were analyzed with GeneChip Operating Software (Affymetrix, Inc.). The expression data were converted to copy numbers of mRNA per cell by the Percellome method, quality controlled, and analyzed using Percellome software [20].

Real-Time PCR Analysis

Real-time PCR was carried out in the iCycler iQ Detection System (Bio-Rad Laboratories) with iQ SYBR-Green Supermix reagents (Bio-Rad Laboratories) as previously described [8]. The PCR amplification reaction was performed with specific primers as shown in Table 1. After PCR, melting-curve analysis was performed to verify specificity and identity of the PCR products. All data were analyzed with the iCycler iQ Optical System Software Version 3.0A (Bio-Rad Laboratories). All PCR data were normalized to *Gapdh* mRNA.

Preparation of Primary Cultured Mesenchymal Cells from UGS

The UGS were dissected from the fetuses and separated into UGE and urogenital sinus mesenchyme (UGM) by tryptic digestion and mechanical separation as previously described [21]. UGM were cultured in RPMI-1640

TABLE 1. Sequences of oligonucleotide primers used for the real-time PCR analyses.

Gene	Primer[a]
Gapdh	F: 5′-AAATGGTGAAGGTCGGTGTG-3′
	R: 5′-TGAAGGGGTCGTTGATGG-3′
Cyp19a1	F: 5′-GCCCAATGAATTTACCCTCGAA-3′
	R: 5′-AAGCCAAAAGGCTGAAAGTACCT-3′
Cyp11a1	F: 5′-TCGACTCCTCAGAACTAAGACCTG-3′
	R: 5′-GTACCCTGGTGTCCTTTATAGCCT-3′
Nr5a1	F: 5′-CCTGGGCTGGCTACCTCTATC-3′
	R: 5′-CGAACTAGAGCCAGAGGAGGAC-3′
Esr1	F: 5′-GCACAGGATGCTAGCCTTGTCTC-3′
	R: 5′-AATTGTCACCAGCTTGCAGGTTC-3′
Ar	F: 5′-GGCGGTCCTTCACTAATGTCAACT-3′
	R: 5′-CTGACTTGTGCATGCGGTACTCAT-3′
Esrrg	F: 5′-CCGAGAGTTGGTGGTTATCATTGG-3′
	R: 5′-GGAAGACCCTCGCCGTGC-3′

[a] F, forward; R, reverse.

with 5% fetal bovine serum and plated out on four-well glass slides (BD Falcon). After several days, cells were fixed in methanol and processed for immunocytochemical analysis.

Immunocytochemical Staining

The sections were first incubated for 15 min in 0.01 M PBS. After inhibition of endogenous peroxidases (10 min in 0.6% H_2O_2 diluted in 0.01 M PBS plus 0.2% Triton X-100 [PBST]) and saturation (2 h in a 5% normal goat serum solution), sections were incubated overnight at 4°C in a polyclonal affinity-purified antiaromatase antibody or estrogen-related receptor gamma (ESRRG) antibody raised in rabbit against quail recombinant aromatase or ESRRG diluted 1:500 in 0.01 M PBST. The next day, the sections were immersed for 2 h at room temperature in a biotin-conjugated goat anti-rabbit immunoglobulin G (DakoCytomation, Inc.) diluted 1:400 in PBST and then for 2 h in a streptavidin-fluorescein complex (Rhodamine; DakoCytomation, Inc.) diluted 1:50 in PBST. Between each step, sections were extensively rinsed in PBST. The sections were mounted onto microscope slides, coverslipped with a gelatin-based mounting medium, and stored in the dark at 4°C. For double-labeling immunofluorescence, Alexa Fluor 488- or 594-conjugated secondary antibodies were used. Rabbit polyclonal anti-aromatase antibody was kindly provided by Prof. Nobuhiro Harada (Department of Biochemistry, Fujita Health University School of Medicine, Aichi, Japan) [22]. The rabbit polyclonal anti-ESRRG antibody used in the present study was established and characterized as previously reported [23]. The mouse monoclonal anti-Ran antibody (Santa Cruz Biotechnology, Inc.) was used to detect nucleus in cells. Ran, also called TC4, is the small RAS-related protein that is localized in the nucleus.

Statistical Analysis

Results are expressed as the mean ± SD. Differences among the three groups were determined using Student *t*-test with Dunnett multiple comparison. A value of $P < 0.05$ was considered to be statistically significant.

RESULTS

BPA-Specific Increases of E_2 Levels and CYP19A1 (Aromatase) Activity in Mouse UGS

The pregnant mice were exposed to low-dose BPA during the onset of prostatic budding (E13–E16), and the UGS of fetuses were collected during bud elongation (E17–P1). In analyses of in situ sex steroid hormonal environment, E_2 levels and CYP19A1 (aromatase) activity were significantly increased only at P1 in BPA-treated UGS, not at P1 in the DES-treated UGS (Fig. 1). At E17 and P1, both the E_2 levels and CYP19A1 (aromatase) activity in untreated male UGS were not significantly different compared with those in untreated female UGS.

BPA-Specific Up-Regulation of Steroidogenic Enzyme and Sex-Determining Gene mRNA in Mouse UGS

To investigate the BPA-specific gene alterations related to increases of the E_2 levels and aromatase activity, we performed preliminary GeneChip analysis with the Percellome method in the BPA- or DES-treated male UGS at E17 and P1. The results showed BPA-specific mRNA up-regulation of steroidogenic enzymes, such as *Cyp11a1*, *Cyp11b1*, and *Cyp17a1*, and sex-determining factors, such as *Nr5a1*, *Nr0b1*, *Gata4*, and *Amhr2* (data not shown). Furthermore, quantitative PCR analysis confirmed the mRNA up-regulation of *Cyp19a1*, *Cyp11a1*, and *Nr5a1* only in the BPA-treated neonatal (P0 and P1) UGS, not in the DES-treated neonatal UGS (Fig. 2). No difference in mRNA expression levels was found between E17 and P1 when comparing the untreated male UGS to that of the female. In

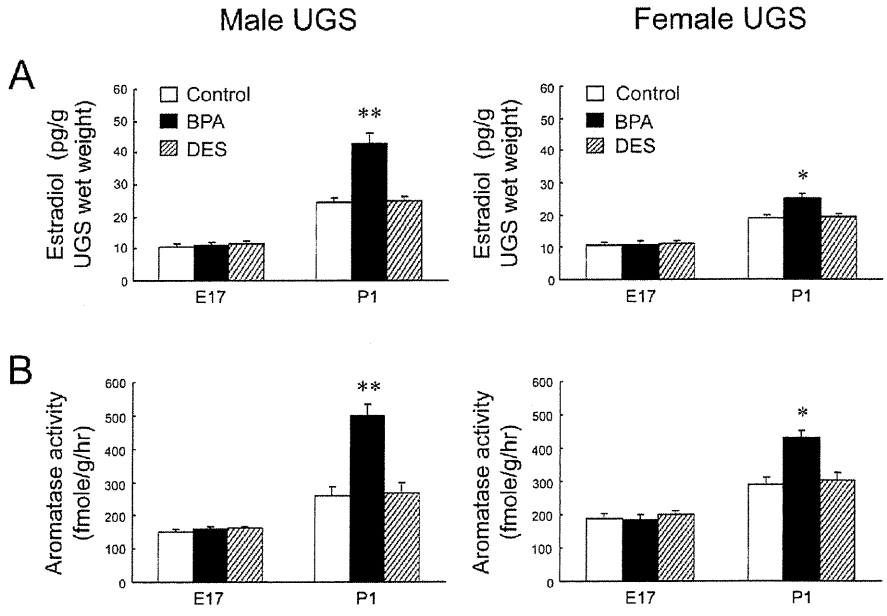

FIG. 1. BPA-specific increases of E_2 levels and CYP19A1 (aromatase) activity in mouse UGS. E_2 levels (**A**) and CYP19A1 (aromatase) activity (**B**) were measured in the untreated control (open bar), BPA-treated UGS (closed bar), and DES-treated UGS (slashed bar) at E17 and P1. $*P < 0.01$, $**P < 0.001$ vs. control.

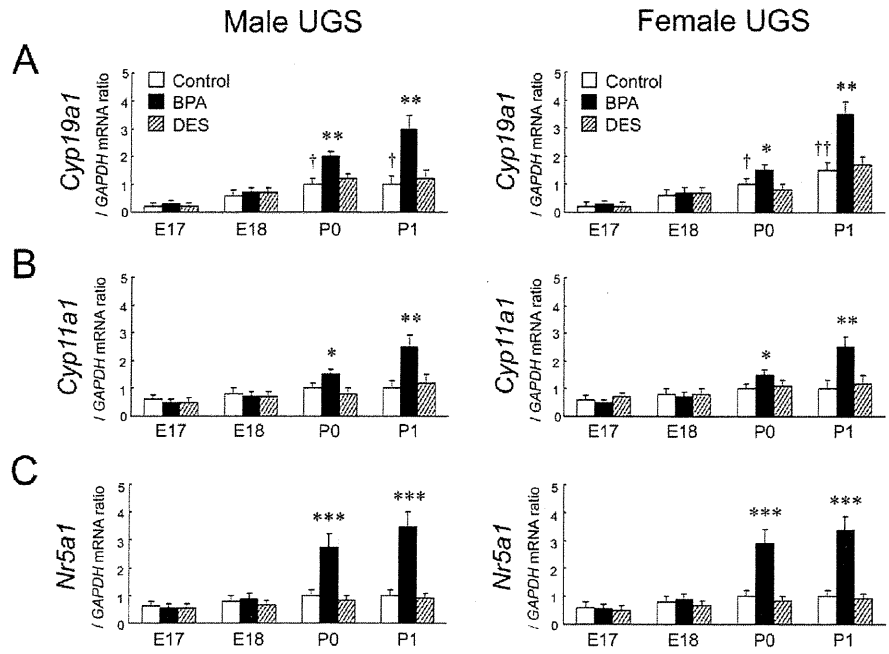

FIG. 2. BPA-specific up-regulation of steroidogenic enzyme and sex-determining gene mRNA in mouse UGS. The relative mRNA expressions of *Cyp19a1* (**A**), *Cyp11a1* (**B**), and *Nr5a1* (**C**) were determined in the untreated control (open bar), BPA-treated UGA (closed bar), and DES-treated UGS (slashed bar) between E17 and P1. $^{*}P < 0.05$, $^{**}P < 0.01$, $^{***}P < 0.001$ vs. control at each time point; $^{\dagger}P < 0.01$, $^{\dagger\dagger}P < 0.001$ vs. control at E17.

untreated male and female UGS, the mRNA of *Cyp19a1* was gradually increased between E17 and P1.

Restricted BPA-Specific Up-Regulation of Steroidogenic Enzyme and Sex-Determining Gene mRNA in UGE and UGM

In male fetuses at P1, it was not feasible to separate UGE and UGM components within the male UGS because of the formation of prostatic buds. In the female at P1, the up-regulation of *Cyp19a1*, *Cyp11a1*, and *Nr5a1* mRNA was observed only in UGM, not in UGE, of the BPA-treated group (Fig. 3). In both male and female UGE, expressions of such mRNAs were quite low and not up-regulated, even in the BPA-treated group. At E17, no difference in mRNA expression levels was found when comparing the untreated male UGM with that of the female.

BPA-Specific Increases of Aromatase-Expressing Cells in Primary Cultured UGM

In both the male and female, P1 UGM was primary cultured in vitro. Representative pictures of aromatase-positive cells are shown in Figure 4, A–C. The aromatase-positive staining was

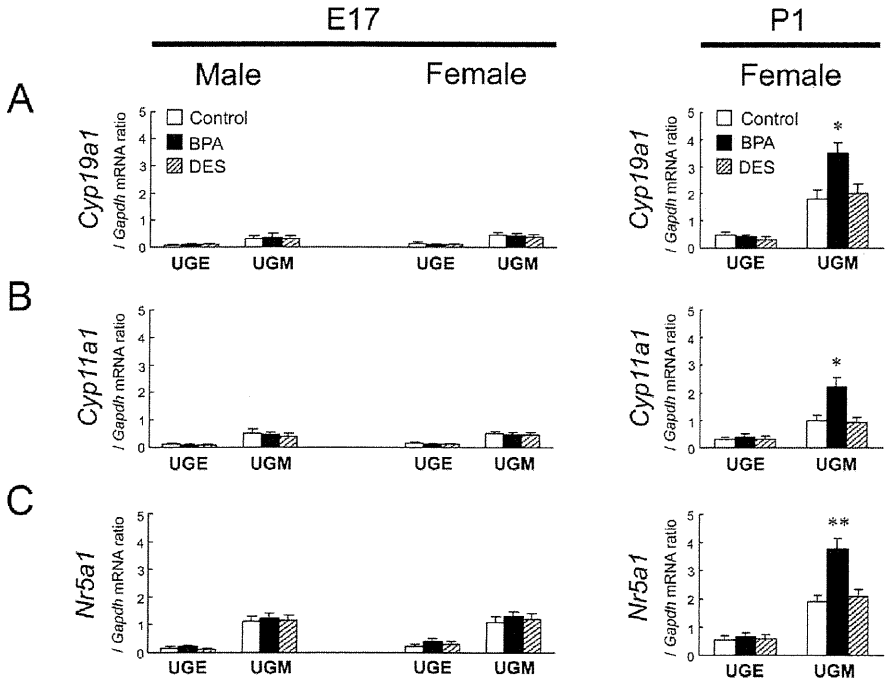

FIG. 3. Restricted BPA-specific up-regulation of steroidogenic enzyme and sex-determining gene mRNA in UGE and UGM. The relative mRNA expressions of *Cyp19a1* (**A**), *Cyp11a1* (**B**), and *Nr5a1* (**C**) were determined for UGE and UGM of the untreated control (open bar), BPA-treated UGS (closed bar), and DES-treated UGS (slashed bar) at E17 and P1. $^{*}P < 0.01$, $^{**}P < 0.001$ vs. control.

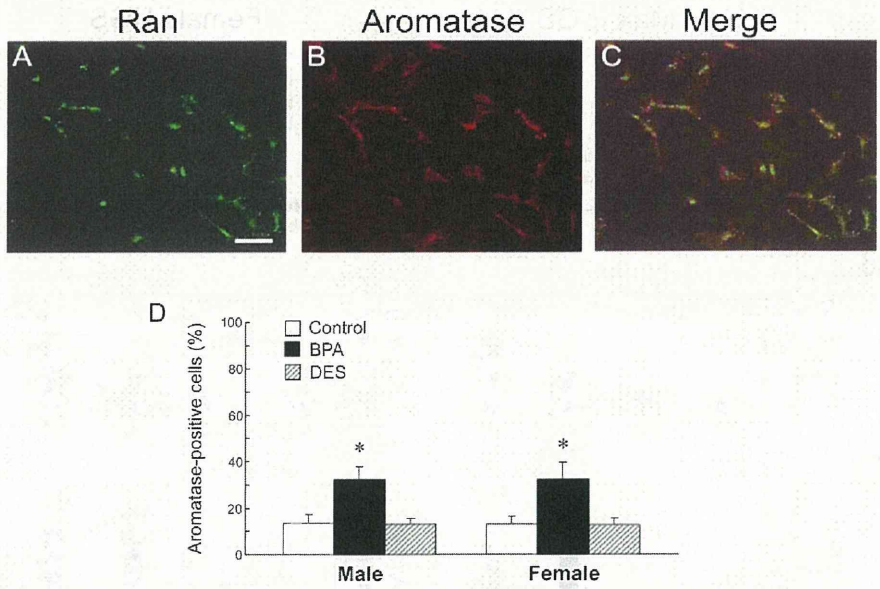

FIG. 4. BPA-specific increases of aromatase-expressing cells in primary cultured UGM. **A–C**) Fluorescence signals were detected for the CYP19A1 (aromatase) protein in primary cultured UGM. The nuclei were identified by Ran staining. Bar = 100 μm, magnification ×400. **D**) The number of aromatase-positive cells was counted in primary cultured UGM of the untreated control open bar), BPA-treated UGS (closed bar), and DES-treated UGS (slashed bar), and the percentage of aromatase-positive cells was calculated from at least 10 areas. *$P < 0.01$ vs. control.

observed in the cytoplasm of cultured UGM. The rate of positivity (i.e., the percentage of cells that expressed CYP19A1 [aromatase] protein), was approximately 10% in the untreated and the DES-treated groups, whereas it was as high as approximately 30% in the BPA-treated group (Fig. 4D). No difference in the rate of positivity of CYP19A1 (aromatase) was found when comparing the untreated male UGM to that of the female.

Restricted BPA-Specific Up-Regulation of Esrrg *mRNA in UGE and UGM*

In E17 female UGM, the mRNA expression of *Esr1* was up-regulated by both BPA and DES treatment (Fig. 5A). At E17, however, the mRNA expression of *Ar* was up-regulated by both BPA and DES treatment in the male UGS (Fig. 5B). At P1, mRNA expression of *Ar* was up-regulated by both BPA and DES treatment in the female UGS (Fig. 5B). In both the male and female, the up-regulation of *Esrrg* mRNA was observed at E17 and restricted in UGM, but not in UGE, of the BPA-treated group (Fig. 5C). In both the male and female UGE, the expression of *Esrrg* mRNA was quite low and not up-regulated, even in the BPA-treated group. At E17, no difference in mRNA expression levels was found when comparing the untreated male UGS with that of the female.

BPA-Specific Increases of ESRRG-Expressing Cells in Primary Cultured UGM

In both the male and female, E17 UGM was primary cultured in vitro. Representative pictures of ESRRG-positive

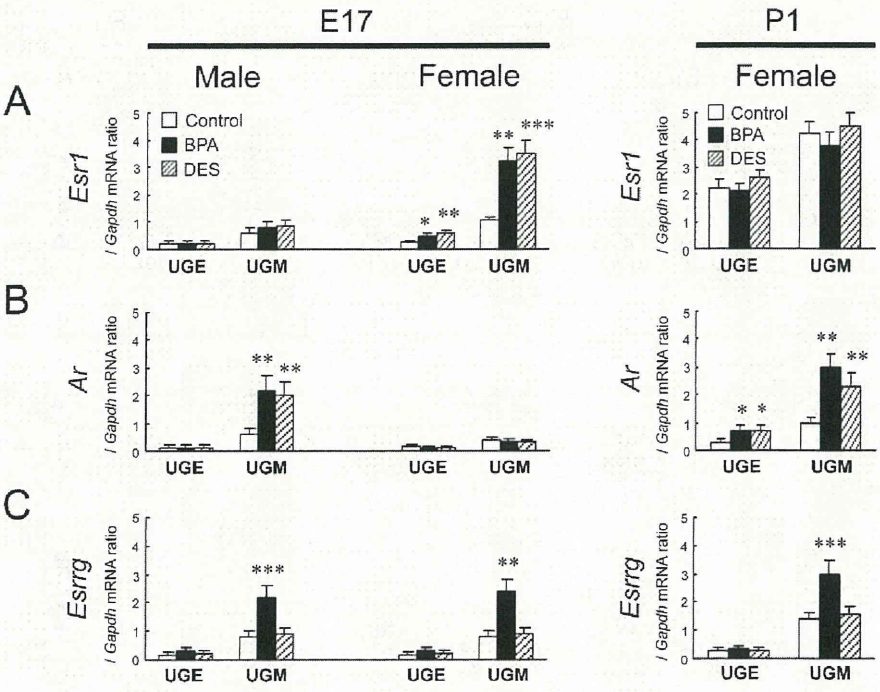

FIG. 5. Restricted BPA-specific up-regulation of *Esrrg* mRNA in UGE and UGM. The relative mRNA expressions of *Esr1* (**A**), *Ar* (**B**), and *Esrrg* (**C**) were determined in UGE and UGM of the untreated control (open bar), BPA-treated UGS (closed bar), and DES-treated UGS (slashed bar) at E17 and P1. *$P < 0.05$, **$P < 0.01$, ***$P < 0.001$ vs. control.

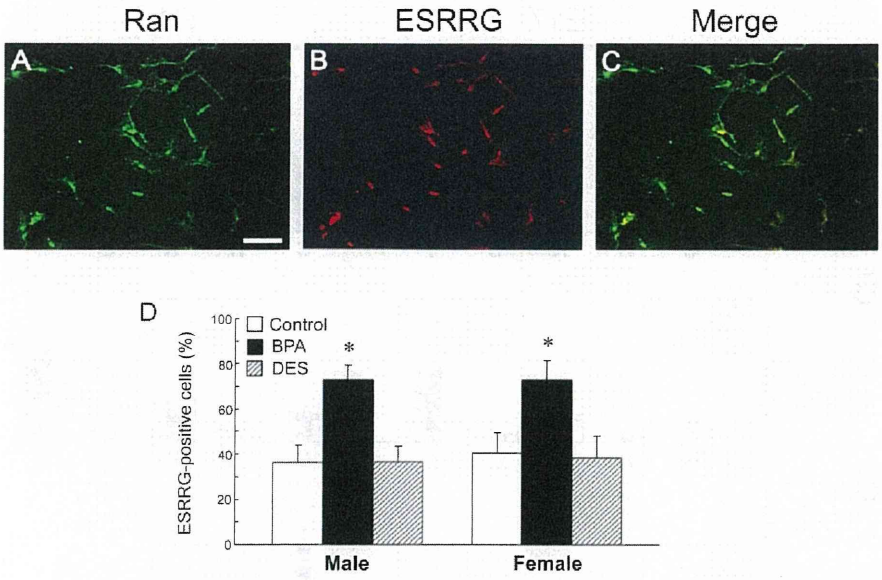

FIG. 6. BPA-specific increases of ESRRG-expressing cells in primary cultured UGM. **A–C**) Fluorescence signals were detected for the ESRRG protein in primary cultured UGM. The nuclei were identified by Ran staining. Bar = 100 μm, magnification ×400. **D**) The number of ESRRG-positive cells was counted in primary cultured UGM of the untreated control (open bar), BPA-treated UGS (closed bar), and DES-treated UGS (slashed bar), and the percentage of ESRRG-positive cells was calculated from at least 10 areas. $*P < 0.01$ vs. control.

cells are shown in Figure 6, A–C. The ESRRG-positive staining was observed in both the nucleus and the cytoplasm of cultured UGM. The number of ESRRG-positive UGM was significantly increased only in the BPA-treated group and showed a 2.2-fold increase in males and a 1.6-fold increase in females (Fig. 6D). No difference was found in the rate of positivity of ESRRG when comparing the untreated male UGM with that of the female.

BPA-Specific Up-Regulation of Esrrg *and Steroidogenic Enzyme mRNA in Sex Hormone-Related Organs*

To investigate the BPA-specific up-regulation of in situ steroidogenesis in other organs, we first examined the changes in *Esrrg* mRNA expression in sex hormone-related organs, such as the cerebellum, heart, kidney, ovary, and testis. At P1, the mRNA expression of *Esr1* in the cerebellum, heart, kidney, and ovary, but not in the testis, was up-regulated by both BPA and DES treatment (Fig. 7A). However, no significant difference in *Ar* mRNA expression was observed in all organs examined (Fig. 7B). In the untreated group, the mRNA expression of *Esrrg* was not detected in the testis at E17 and P1 (Fig. 7C). The up-regulation of *Esrrg* mRNA was observed at E17 and restricted to the cerebellum, heart, kidney, and ovary (Fig. 7C). The BPA-specific up-regulation of *Cyp19a1*, *Cyp11a1*, and *Nr5a1* mRNA was observed only at P1 in the cerebellum, heart, kidney, and ovary, but not in the testis (Fig. 8).

DISCUSSION

Concern about the effects of EDCs such as BPA on human health has been increasing [24]. Although the majority of EDCs have the potential to alter functioning of the reproductive and endocrine system, the actual mechanism responsible for such alterations has not been identified thoroughly. BPA is of concern because its chemical structure resembles that of DES. Several studies have reported that BPA can mimic estrogen action, such as induction of vaginal cornification, uterine vascular permeability, growth and differentiation of the mammary gland, and synaptic plasticity in the hippocampus [25–28]. In the prostate, alterations in normal development can produce permanent changes that persist throughout adulthood and may increase the risk of disease in later life [9]. Thus, our objective was to investigate the biological effects of low-dose BPA on the initial development of primary ducts in the fetal prostate.

During prostatic development, alteration of sex steroid hormone synthesis may be responsible for prostatic anomalies associated with fetal exposure to EDCs. In the present study, fetal exposure to low-dose BPA increased E_2 levels in P1 UGS of both the male and female, whereas DES-induced changes were not detected. This alteration was also correlated with increased activity of CYP19A1 (aromatase) in UGS at P1, suggesting the unique action of BPA for in situ steroidogenesis in UGS. The BPA-specific increase of E_2 levels in UGS at P1 was correlated with the following: mRNA up-regulation of steroidogenic enzymes, such as *Cyp19a1* and *Cyp11a1*, and an increased number of aromatase-expressing UGM. The enzyme CYP19A1 (aromatase) is responsible for in situ E_2 production and the crucial testosterone/E_2 balance necessary for normal embryonic and fetal development, even in males. The data presented here shows that the up-regulation of *Cyp19a1* mRNA in BPA-treated UGM was comparable to changes in both in situ E_2 production and CYP19A1 (aromatase) activity.

In the present study, we demonstrated that the BPA-specific increase in steroidogenic enzyme mRNA and aromatase-expressing cell number were observed in both the male and female UGM. During embryonic development, the mesenchymal component is involved in the induction and organogenesis of various organs, including the prostate, mammary gland, lung, kidney, and pancreas. It has been well established that subpopulations of the mesenchymal component are a source of potent molecules that regulate epithelial growth and differentiation [29]. In the prostate, androgen-responsive signals derived from UGM permissively and instructively induce UGE to form primary ducts of the prostate [30].

Comparison between the neonatal male and female UGS shows a similarity in the condensed mesenchyme of the ventral areas—that is, the ventral prostate mesenchyme (VPM) in the male and the ventral mesenchymal pad (VMP) in the female [31]. In the male, a defined VPM is specifically associated with ductal branching morphogenesis and cytodifferentiation of the ventral prostate. Females do not usually form a prostate. In a

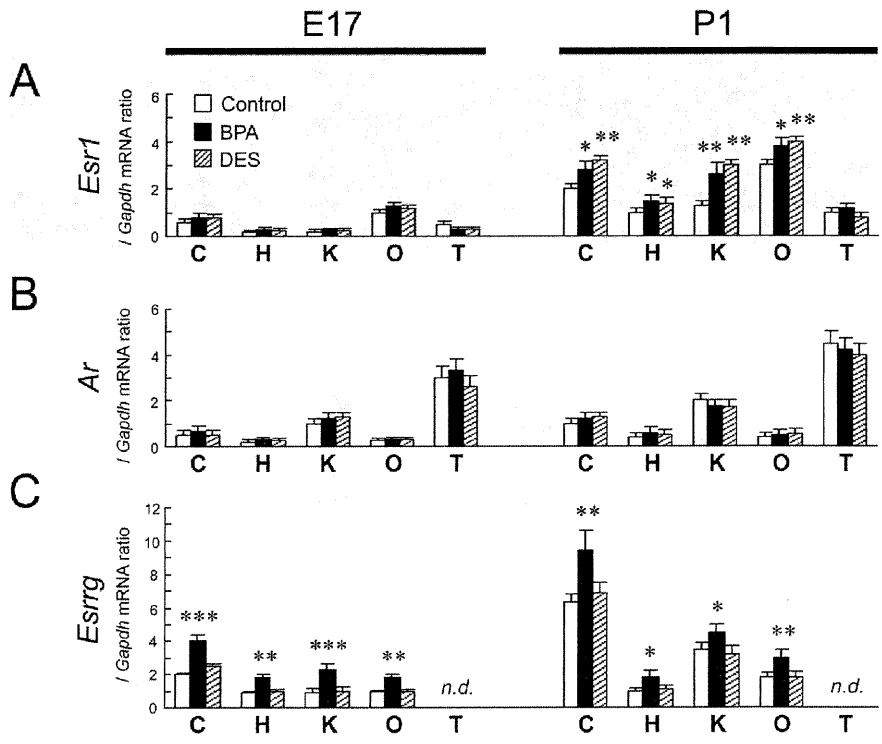

FIG. 7. BPA-specific up-regulation of *Esrrg* mRNA in sex steroid hormone-related organs. The relative mRNA expressions of *Esr1* (**A**), *Ar* (**B**), and *Esrrg* (**C**) were determined in sex steroid hormone-related organs of the untreated control (open bar), BPA-treated UGS (closed bar), and DES-treated UGS (slashed bar) at E17 and P1. C, cerebellum; H, heart; K, kidney; O, ovary; T, testis; *n.d.*, not detected. $^{*}P < 0.05$, $^{**}P < 0.01$, $^{***}P < 0.001$ vs. control.

tissue recombination model, the female VMP induces prostate development in response to androgens [32], suggesting that cells within the female VMP have prostatic-inductive activity. Moreover, an earlier tissue recombination study showed that the ability of the female UGS to respond to androgens in forming prostate was gradually lost between P1 and P5 [33]. These results suggest strongly that androgen-responsive regulatory molecules are expressed constitutively even in the female VMP. Although the female VMP forms in the absence of androgens, androgen receptor (AR) expression was observed in the neonatal female VMP in a pattern similar to that observed in the male VPM [34]. Therefore, the BPA-specific increase in E_2 levels might interact with the intracellular AR signaling in both the male VPM and the female VMP. However, to our knowledge,

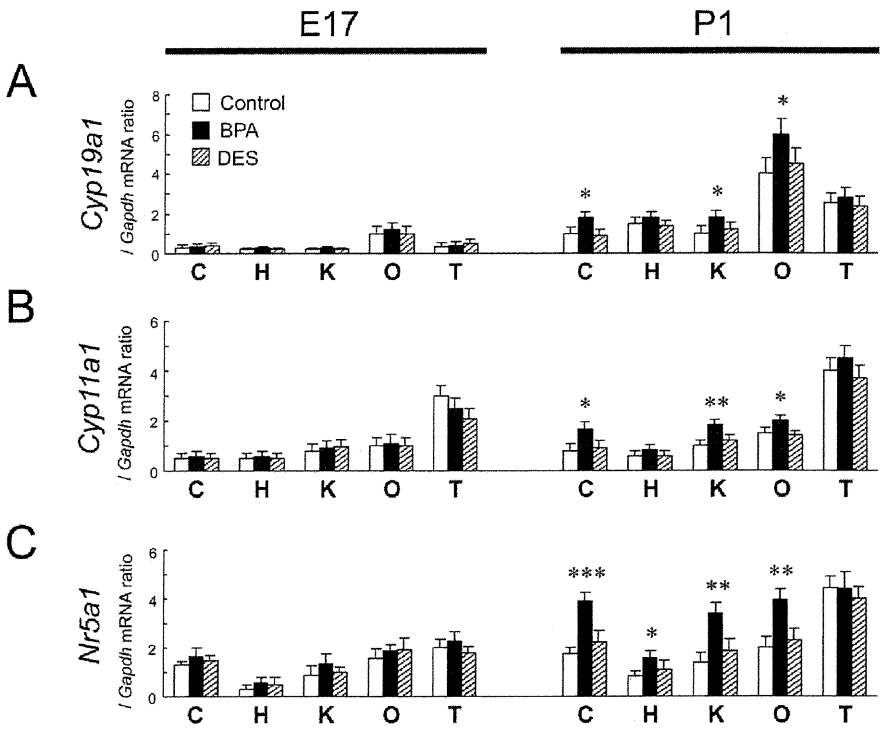

FIG. 8. BPA-specific up-regulation of steroidogenic enzyme and sex-determining gene mRNA in sex steroid hormone-related organs. The relative mRNA expressions of *Cyp19a1* (**A**), *Cyp11a1* (**B**), and *Nr5a1* (**C**) were determined in sex steroid hormone-related organs of the untreated control (open bar), BPA-treated UGS (closed bar), and DES-treated UGS (slashed bar) at E17 and P1. C, cerebellum; H, heart; K, kidney; O, ovary; T, testis. $^{*}P < 0.05$, $^{**}P < 0.01$, $^{***}P < 0.001$ vs. control.

the morphological changes in neonatal female UGS have not yet been investigated.

Our results suggest that BPA has a stimulatory effect on in situ steroidogenesis in P1 UGS of both the male and female at low-dose exposure levels. Recently, ESRRG has been reported to bind strongly with BPA [35]. Susens et al. [36] have reported that expression of ESRRG in the mouse is organ-specific: ESRRG is expressed in the brain, heart, kidney, and skeletal muscle but not in the lung, spleen, and testis. In the present study, the up-regulation of *Cyp19a1* and *Cyp11a1* mRNA by BPA treatment was detected only in organs expressing *Esrrg* mRNA. These data suggest that the possibility of a stimulatory effect on in situ steroidogenesis by fetal exposure to low-dose BPA may be a concern not only in UGS but also in organs expressing ESRRG, such as the brain, heart, kidney, and ovary. It is important to note that Takeda et al. [23] have recently reported that ESRRG was detected in the human testis, suggesting that the distribution of ESRRG differs slightly between mice and humans.

In the present study, the BPA-specific up-regulation of steroidogenic enzyme mRNA in UGS, cerebellum, heart, kidney, and ovary was observed only during the neonatal period (i.e., P0 and P1) and not during the prenatal period (i.e., E17 and E18). During pregnancy in rodents, large amounts of estrogens produced in the maternal ovaries are continuously delivered to the fetus through the placenta. After birth, however, the fetus may be released from the maternal, high-estrogen environment. Thus, one possibility is that the maternal, high-estrogen environment in pregnancy may protect the fetus from the effect of BPA on in situ steroidogenesis during the prenatal period. However, we did not investigate the effects of neonatal BPA treatment on in situ steroidogenesis.

The EDC-induced alterations of the in situ estrogen environment depend on each compound. In addition to atrazine and dioxin, the organotin compound tributyltin also increases E_2 production in human placental choriocarcinoma cells [37]. Tributyltin has been demonstrated to induce the superimposition of male sex organs, such as a penis and/or a vas deferens, over female sex organs, which is a phenomenon known as imposex [38]. These studies suggest strongly that EDCs might affect fetal development not only by mimicking the actions of sex steroid hormones but also by alteration of in situ steroidogenesis.

In the prostate, AR expressed in mesenchyme is required for directing growth and branching morphogenesis of epithelia, presumably by induction of growth factors [39]. In the present study, fetal exposure to BPA or DES increased *Ar* mRNA expression in E17 UGM of the male, whereas *Esr1* mRNA expression was up-regulated in E17 UGM of the female. Recently, Richter et al. [40] have reported that in vitro BPA treatment stimulates *Ar* and *Esr1* mRNA expression in mesenchymal cells isolated from fetal mouse prostate. Thus, our results support the idea that BPA-induced cell proliferation of the primary prostatic ducts may be caused by inducing *Ar* mRNA expression in the male UGM. In contrast, the induction of *Esr1* mRNA expression by BPA or DES may create a positive-feedback loop in the female UGM. Further investigation and morphological analysis will be necessary to confirm the effects of up-regulated ESR1 in the female UGS.

In conclusion, we have shown the unique action of BPA in the mouse UGS. Specifically, we have demonstrated that the increases in E_2 levels and CYP19A1 (aromatase) activity were observed in the BPA-treated UGS but not in the DES-treated UGS. Ricke et al. [41] have recently reported that stromal hormone imbalance, a potential source of local E_2 production, may be responsible for prostatic disease, such as benign prostatic hyperplasia and prostate cancer. The data in the present study give rise to the concept that the development and differentiation of UGS in mouse fetuses is very sensitive to fetal exposure to low-dose BPA via the mother. Further investigation of various aspects of BPA-specific action is necessary to fully understand the role of BPA as an EDC.

ACKNOWLEDGMENTS

We thank Prof. Nobuhiro Harada at Department of Biochemistry, Fujita Health University School of Medicine, Aichi, Japan, for kindly providing rabbit polyclonal antiaromatase antibody. We also thank Mrs. Hiroko Nishii for technical support.

REFERENCES

1. Sekizawa J. Low-dose effects of bisphenol A: a serious threat to human health? J Toxicol Sci 2008; 33:389–403.
2. Newbold RR, Jefferson WN, Padilla-Banks E. Prenatal exposure to bisphenol A at environmentally relevant doses adversely affects the murine female reproductive tract later in life. Environ Health Perspect 2009; 117:879–885.
3. McPherson SJ, Ellem SJ, Risbridger GP. Estrogen-regulated development and differentiation of the prostate. Differentiation 2008; 76:660–670.
4. Welshons WV, Nagel SC, vom Saal FS. Large effects from small exposures. III. Endocrine mechanisms mediating effects of bisphenol A at levels of human exposure. Endocrinology 2006; 147:S56–S69.
5. Schonfelder G, Wittfoht W, Hopp H, Talsness CE, Paul M, Chahoud I. Parent bisphenol A accumulation in the human maternal-fetal-placental unit. Environ Health Perspect 2002; 110:A703–A707.
6. Tsutsumi O. Assessment of human contamination of estrogenic endocrine-disrupting chemicals and their risk for human reproduction. J Steroid Biochem Mol Biol 2005; 93:325–330.
7. Timms BG, Howdeshell KL, Barton L, Bradley S, Richter CA, vom Saal FS. Estrogenic chemicals in plastic and oral contraceptives disrupt development of the fetal mouse prostate and urethra. Proc Natl Acad Sci U S A 2005; 102:7014–7019.
8. Ogura Y, Ishii K, Kanda H, Kanai M, Arima K, Wang Y, Sugimura Y. Bisphenol A induces permanent squamous change in mouse prostatic epithelium. Differentiation 2007; 75:745–756.
9. Ho SM, Tang WY, Belmonte de Frausto J, Prins GS. Developmental exposure to estradiol and bisphenol A increases susceptibility to prostate carcinogenesis and epigenetically regulates phosphodiesterase type 4 variant 4. Cancer Res 2006; 66:5624–5632.
10. Markey CM, Luque EH, Munoz de Toro M, Sonnenschein C, Soto AM. In utero exposure to bisphenol A alters the development and tissue organization of the mouse mammary gland. Biol Reprod 2001; 65: 1215–1223.
11. Honma S, Suzuki A, Buchanan DL, Katsu Y, Watanabe H, Iguchi T. Low-dose effect of in utero exposure to bisphenol A and diethylstilbestrol on female mouse reproduction. Reprod Toxicol 2002; 16:117–122.
12. Kubo K, Arai O, Omura M, Watanabe R, Ogata R, Aou S. Low-dose effects of bisphenol A on sexual differentiation of the brain and behavior in rats. Neurosci Res 2003; 45:345–356.
13. Fan W, Yanase T, Morinaga H, Gondo S, Okabe T, Nomura M, Komatsu T, Morohashi K, Hayes TB, Takayanagi R, Nawata H. Atrazine-induced aromatase expression is SF-1 dependent: implications for endocrine disruption in wildlife and reproductive cancers in humans. Environ Health Perspect 2007; 115:720–727.
14. Baba T, Mimura J, Nakamura N, Harada N, Yamamoto M, Morohashi K, Fujii-Kuriyama Y. Intrinsic function of the aryl hydrocarbon (dioxin) receptor as a key factor in female reproduction. Mol Cell Biol 2005; 25: 10040–10051.
15. Moustafa GG, Ibrahim ZS, Hashimoto Y, Alkelch AM, Sakamoto KQ, Ishizuka M, Fujita S. Testicular toxicity of profenofos in matured male rats. Arch Toxicol 2007; 81:875–881.
16. Song KH, Lee K, Choi HS. Endocrine disrupter bisphenol A induces orphan nuclear receptor Nur77 gene expression and steroidogenesis in mouse testicular Leydig cells. Endocrinology 2002; 143:2208–2215.
17. Mlynarcikova A, Kolena J, Fickova M, Scsukova S. Alterations in steroid hormone production by porcine ovarian granulosa cells caused by bisphenol A and bisphenol A dimethacrylate. Mol Cell Endocrinol 2005; 244:57–62.
18. Hojo Y, Higo S, Ishii H, Ooishi Y, Mukai H, Murakami G, Kominami T, Kimoto T, Honma S, Poirier D, Kawato S. Comparison between

hippocampus-synthesized and circulation-derived sex steroids in the hippocampus. Endocrinology 2009; 150:5106–5112.
19. Nakanishi T, Nishikawa J, Hiromori Y, Yokoyama H, Koyanagi M, Takasuga S, Ishizaki J, Watanabe M, Isa S, Utoguchi N, Itoh N, Kohno Y, et al. Trialkyltin compounds bind retinoid X receptor to alter human placental endocrine functions. Mol Endocrinol 2005; 19:2502–2516.
20. Kanno J, Aisaki K, Igarashi K, Nakatsu N, Ono A, Kodama Y, Nagao T. "Per cell" normalization method for mRNA measurement by quantitative PCR and microarrays. BMC Genomics 2006; 7:64–77.
21. Ishii K, Imanaka-Yoshida K, Yoshida T, Sugimura Y. Role of stromal tenascin-C in mouse prostatic development and epithelial cell differentiation. Dev Biol 2008; 324:310–319.
22. Jakab RL, Horvath TL, Leranth C, Harada N, Naftolin F. Aromatase immunoreactivity in the rat brain: gonadectomy-sensitive hypothalamic neurons and an unresponsive "limbic ring" of the lateral septum-bed nucleus-amygdala complex. J Steroid Biochem Mol Biol 1993; 44:481–498.
23. Takeda Y, Liu X, Sumiyoshi M, Matsushima A, Shimohigashi M, Shimohigashi Y. Placenta expressing the greatest quantity of bisphenol A receptor ERRgamma among the human reproductive tissues: predominant expression of type-1 ERRgamma isoform. J Biochem 2009; 146:113–122.
24. vom Saal FS, Akingbemi BT, Belcher SM, Birnbaum LS, Crain DA, Eriksen M, Farabollini F, Guillette LJ Jr, Hauser R, Heindel JJ, Ho SM, Hunt PA, et al. Chapel Hill Bisphenol A Expert Panel Consensus Statement: integration of mechanisms, effects in animals and potential to impact human health at current levels of exposure. Reprod Toxicol 2007; 24:131–138.
25. Steinmetz R, Mitchner NA, Grant A, Allen DL, Bigsby RM, Ben-Jonathan N. The xenoestrogen bisphenol A induces growth, differentiation, and c-fos gene expression in the female reproductive tract. Endocrinology 1998; 139:2741–2747.
26. Milligan SR, Balasubramanian AV, Kalita JC. Relative potency of xenobiotic estrogens in an acute in vivo mammalian assay. Environ Health Perspect 1998; 106:23–26.
27. Colerangle JB, Roy D. Profound effects of the weak environmental estrogen-like chemical bisphenol A on the growth of the mammary gland of Noble rats. J Steroid Biochem Mol Biol 1997; 60:153–160.
28. Kawato S. Endocrine disrupters as disrupters of brain function: a neurosteroid viewpoint. Environ Sci 2004; 11:1–14.
29. Donjacour AA, Cunha GR. Stromal regulation of epithelial function. Cancer Treat Res 1991; 53:335–364.
30. Hayashi N, Cunha GR, Parker M. Permissive and instructive induction of adult rodent prostatic epithelium by heterotypic urogenital sinus mesenchyme. Epithelial Cell Biol 1993; 2:66–78.
31. Thomson AA. Role of androgens and fibroblast growth factors in prostatic development. Reproduction 2001; 121:187–195.
32. Timms BG, Lee CW, Aumuller G, Seitz J. Instructive induction of prostate growth and differentiation by a defined urogenital sinus mesenchyme. Microsc Res Tech 1995; 30:319–332.
33. Cunha GR. Age-dependent loss of sensitivity of female urogenital sinus to androgenic conditions as a function of the epithelia-stromal interaction in mice. Endocrinology 1975; 97:665–673.
34. Thomson AA, Timms BG, Barton L, Cunha GR, Grace OC. The role of smooth muscle in regulating prostatic induction. Development 2002; 129: 1905–1912.
35. Takayanagi S, Tokunaga T, Liu X, Okada H, Matsushima A, Shimohigashi Y. Endocrine disruptor bisphenol A strongly binds to human estrogen-related receptor gamma (ERRgamma) with high constitutive activity. Toxicol Lett 2006; 167:95–105.
36. Susens U, Hermans-Borgmeyer I, Borgmeyer U. Alternative splicing and expression of the mouse estrogen receptor-related receptor gamma. Biochem Biophys Res Commun 2000; 267:532–535.
37. Nakanishi T, Kohroki J, Suzuki S, Ishizaki J, Hiromori Y, Takasuga S, Itoh N, Watanabe Y, Utoguchi N, Tanaka K. Trialkyltin compounds enhance human CG secretion and aromatase activity in human placental choriocarcinoma cells. J Clin Endocrinol Metab 2002; 87:2830–2837.
38. Horiguchi T. Masculinization of female gastropod mollusks induced by organotin compounds, focusing on mechanism of actions of tributyltin and triphenyltin for development of imposex. Environ Sci 2006; 13:77–87.
39. Cunha GR, Donjacour A. Stromal-epithelial interactions in normal and abnormal prostatic development. Prog Clin Biol Res 1987; 239:251–272.
40. Richter CA, Taylor JA, Ruhlen RL, Welshons WV, Vom Saal FS. Estradiol and bisphenol A stimulate androgen receptor and estrogen receptor gene expression in fetal mouse prostate mesenchyme cells. Environ Health Perspect 2007; 115:902–908.
41. Ricke WA, McPherson SJ, Bianco JJ, Cunha GR, Wang Y, Risbridger GP. Prostatic hormonal carcinogenesis is mediated by in situ estrogen production and estrogen receptor alpha signaling. FASEB J 2008; 22: 1512–1520.

Social engineering for virtual 'big science' in systems biology

Hiroaki Kitano, Samik Ghosh & Yukiko Matsuoka

A new type of big science is emerging that involves knowledge integration and collaboration among small sciences. Because open collaboration involves participants with diverse motivations and interests, social dynamics have a critical role in making the project successful. Thus, proper 'social engineering' will have greater role in scientific project planning and management in the future.

Scientific projects with large amounts of funding to achieve a defined mission are often referred to as 'big science'. Successful big science projects should have a clearly defined goal, a possible means to achieve it and a strong sociological rationale to justify public funding of such endeavors. Similarly, the type of project that can be widely supported beyond the scientific community depends on societal needs at the time.

Although most biology has been and continues to be small science, the Human Genome Project and other genome projects are considered big science in biology. A defining feature of these projects is a large-scale engineering effort designed in support of a specific scientific aim. Projects involving particle colliders and genome sequencing are essentially equipment-driven data-acquisition projects, and such projects will continue to provide new findings through equipment advances.

There is a related desire to obtain a comprehensive understanding of specific cellular systems and biological processes through high-throughput methods. Emergence of systems biology as mainstream biology is accelerating this tendency, because it often requires measurements and analysis of various large-scale and multifaceted data. At the same time, new knowledge critical for in-depth and precise understanding of systems is often derived from small science. This means that a new type of big science is needed that consolidates data and knowledge not only from large-scale projects, but also from discoveries by small science.

It is therefore inevitable that a 'virtual' big science will form, connecting large numbers of researchers around the globe to attain large-scale knowledge integration in an emergent manner. The implication is that such an initiative must have widely acceptable objectives, leadership and proper sociological design to make it sustainable.

There is an impossible number of problems that have yet to be resolved in the biomedical field, and some of these would benefit from being included in big science projects, either in a deliberate and organized or in a more emergent manner. For example, in the numerous cases of diseases for which effective cures are not available but are being proposed and developed, problems remain. Indeed, the cost of drug discovery is so high that it puts severe pressure on the public medical system and impedes access to drugs for underprivileged segments, which in turn prevents development of drugs for rare diseases or those that are prevalent in the poorest areas of the world.

The rising cost of drug discovery affects all segments of society. With increased understanding of individual genomic variations and their impacts on drug efficacy and side effects, we can envision an era of personalized medicine in which patients are selected on the basis of genetic and biochemical differences that underlie different responses to drugs. This would help patients minimize side effects and help health-care systems eliminate considerable misdirected cost. At the same time, it may also mean substantial revenue reduction for pharmaceutical companies. Research and development (R&D) as an industry, and thereby the ability to find possible cures for orphan diseases, may not be sustainable unless drastic reductions in R&D costs are achieved.

Cost and access to medical services is a critical factor for the base-of-the-pyramid segment of the population. For example, tuberculosis is still a major killer in developing countries, as 9.27 million new infections were reported in 2007 globally, with a significant percentage of them being multidrug resistant and some being extensively drug resistant[1]. Yet only a handful of drug-discovery projects exist because of the mismatch between the investment of R&D and the ability of countries where tuberculosis is prevalent to afford treatment. Unless cost-effective drug development can be achieved, those who suffer from neglected diseases will not be saved. Developing technologies to substantially mitigate these problems is socially valuable.

Knowledge integration at all levels

One of the fundamental causes of low productivity in drug discovery is a lack of in-depth understanding of the complexity of biological systems and a means of predicting potential outcomes of candidate compounds when used in cells, model animals and patients (http://www.fda.gov/downloads/ScienceResearch/SpecialTopics/CriticalPathInitiative/CriticalPathOpportunitiesReports/ucm113411.pdf and http://www.pwc.com/gx/en/pharma-life-sciences/pharma-2020/pharma-2020-vision-path.jhtml). Proper introduction of a system- and network-oriented approach to drug discovery, with prediction capabilities even at the cellular level, is expected to rectify the situation by providing a better understanding of the biology that underlies diseases and, ultimately, by enabling us to use precise computational models of cells, organs and patients. Already, several systems biology efforts are under way and being planned.

Development of precise biological models requires integration of knowledge and data at all levels, from genomics and proteomics to imaging and physiology. Various data from high-throughput experiments provide us with genome-wide characteristics, but small-sciences data must be incorporated to gain an understanding of the detailed mechanisms. For both financial and sociological reasons, no single large-scale project can address a systems-level problem truly comprehensively. For instance, even if a large-scale project is